



Journal of the Serbian *el*ectronic Chemical Society

JSCS-info@shd.org.rs • www.shd.org.rs/JSCS

ACCEPTED MANUSCRIPT

This is an early electronic version of an as-received manuscript that has been accepted for publication in the Journal of the Serbian Chemical Society but has not yet been subjected to the editing process and publishing procedure applied by the JSCS Editorial Office.

Please cite this article as S. Meshram, A. N. Joshi, G. P. Dewangan, C. Thakur, and A. B. Soni, *J. Serb. Chem. Soc.* (2026) <https://doi.org/10.2298/JSC250819003M>

This “raw” version of the manuscript is being provided to the authors and readers for their technical service. It must be stressed that the manuscript still has to be subjected to copyediting, typesetting, English grammar and syntax corrections, professional editing and authors’ review of the galley proof before it is published in its final form. Please note that during these publishing processes, many errors may emerge which could affect the final content of the manuscript and all legal disclaimers applied according to the policies of the Journal.



Adsorptive removal of Pb(II) from industrial effluent using nitric acid modified activated carbon: Optimization using Taguchi method

SAURABH MESHRAM^{1*}, ANURADHA N JOSHI¹, GAUTAM PRASAD DEWANGAN¹,
CHANDRAKANT THAKUR² AND ANUPAM B. SONI²

¹Department of Chemical Engineering, Guru Ghasidas Vishwavidyalaya, Bilaspur, 495009, Chhattisgarh, India, and ²Department of Chemical Engineering, National Institute of Technology Raipur, 492010, Chhattisgarh, India.

(Received 19 August; revised 22 October; accepted 25 December 2025)

Abstract: The study aimed to examine the use of nitric acid modified granular activated carbon to treat the wastewater of lead-acid battery recycling unit for lead removal. The adsorbent was characterized using FTIR, SEM, and XRD analysis. Surface functional groups, surface morphology and crystallinity has been changed due to modification. The batch adsorption study was conducted to evaluate the effects of adsorbent dose, initial pH, and contact time on adsorption performance for lead removal. Experiments were performed according to Taguchi design of experiment method and factors were optimized based on SNR analysis to maximize the response. The ideal factor values were found as pH 6, adsorbent dose of 0.05 g, and time of 240 minutes for the adsorption of lead onto adsorbent with the adsorbent uptake capacity of 9.93 mg g⁻¹. From ANOVA analysis pH was found most significant factor with F-value of 28.07. Isotherm and kinetic studies were also carried out to understand the mechanism of adsorption. Adsorption was found to follow the Langmuir isotherm and second order kinetic model.

Keywords: lead-acid battery; Taguchi optimization; adsorption; granular activated carbon; impregnation.

INTRODUCTION

Recycling of lead-acid batteries (LAB) is a crucial source of lead (Pb) for storage battery production and also protects the environment. However, the recycling process generates wastewater with a pH of 1-1.5 and Pb concentrations ranging from 2 to 300 mg L⁻¹.¹ If this effluent is discharged untreated, it may adversely affect soil fertility and groundwater quality. If enters in the food chain, Pb may interfere with working of major systems of human body such as nervous system, digestive system, reproductive system, and urinary system by affecting

* Corresponding author. E-mail: saurabhmeshram88@gmail.com
<https://doi.org/10.2298/JSC250819003M>

major organs.² Conventionally, sodium carbonate is used to desulfurize and neutralize the effluent, separating the lead in the form of sludge.³ According to a 2011 market survey report by the Mineral Economics Division, Indian Bureau of Mines, there were only 316 registered recyclers in India in 2010, including five in Chhattisgarh state. However, many backyard smelters dispose of the effluent without any treatment to gain profit. These smelters require an efficient and inexpensive technique to treat the effluent and keep the Pb(II) concentration in the discharge within safe limits (0.1 mg L⁻¹).

Various methods are available to remove Pb(II) from water such as precipitation, membrane separation, ion exchange, electrocoagulation, filtration, and adsorption.⁴ Adsorption is a widely used technique due to its easy operational and economical nature and low capital cost. Activated carbon is often used in water treatment processes due to its different chemical characteristics, porous structure, and high surface area.⁵ Activated carbon is available in both powder (PAC) and granular (GAC) forms, with PAC having larger pores and GAC having smaller internal pores and a lower adsorption rate than PAC. GAC is preferred over PAC due to its ease of handling and disposal and lower loss during operation.⁶ Several investigations have utilized GAC to treat wastewater, including removing lead from aqueous solutions by Dwivedi *et al.*, removing copper, zinc, and lead ions by Chen and Wang, removing amoxicillin from water by Franco *et al.*, removing phenol from synthetic water by Sulaymon *et al.*, and removing cadmium and lead by Jusoh *et al.*⁶⁻¹⁰

Activated carbon is a widely used adsorbent to treat water because of the properties such as porous structure, abundant active sites, functional groups, and high surface area. However, its adsorption capacity is limited, and researchers have modified it using chemical agents to enhance its efficiency by promoting chemisorption of pollutants on the surface. Wang *et al.* modified GAC by using magnesium, resulting in an increased adsorption capacity from 3.47 to 8.08 mg g⁻¹ for the adsorption of Cd(II).¹¹ Fan and Anderson used the oxide of Mn for the retrieval of Cu(II) and Cd(II), and Yao *et al.* modified activated carbon made of rice husk using nitric acid, which increased its uptake capacity by improving the surface characteristics and porous structure.^{12,13} In another study, Jiang *et al.* found that modifying activated carbon with HNO₃ as an impregnating agent after oxidizing it using concentrated sulfuric acid increased the mesoporous volume, specific surface area, and uptake capacity for the separation of dibenzothiophene and methylene blue.¹⁴

The modification of activated carbon with nitric acid is already studied, this study investigates the effect of modification on granular activated carbon. HNO₃-modified GAC was used unprecedently as an adsorbent for treatment of LAB recycling unit effluent. The characteristics of GAC and HNGAC were analysed using SEM, FTIR, and XRD to determine the effect of modification. The

experimental run of adsorption was conducted based on Taguchi orthogonal L16 array (4^3) with four levels of parameters adsorbent dose, retention time, and pH. The parameters were optimized using signal-to-noise ratio (SNR) obtained from Taguchi analysis.

EXPERIMENTAL

Wastewater

The wastewater of lead-acid battery (LAB) recycling plant was obtained from a smelter in Raipur, Chhattisgarh, India. The pH of the effluent was 1.2 and concentration of Pb(II) was 11.2 mg L⁻¹. Prior to the batch adsorption study, the pH of the wastewater was adjusted using standard solutions of sodium hydroxide and hydrochloride.

Adsorbent

Granular activated carbon (GAC) was commercially procured and improved using nitric acid following the process described by El-Wakil *et al.*¹⁵ To prepare the modified GAC, a mixture of HNO₃ and distilled water in a 1:1 ratio was heated to 110 °C. Then, 1 g of GAC was added to 5 mL of the boiled solution and heated for 3 hours. The resulting solution was filtered, and the solid part was collected and washed with distilled water until the pH reached 6. Finally, the nitric acid modified GAC (HNGAC) was dried for 24 hours at 100 °C in hot air oven.

Characterization

The surface functional groups of the adsorbents were analyzed using FTIR (Bruker, Alpha Model) within the 4000-400 cm⁻¹ range of wavelength. The ZEISS EVO Series Scanning Electron Microscope (SEM) Model was used to obtain surface micrographs and element percentage of the adsorbents before and after the modification with the nitric acid. PANalytical multifunctional XRD analyzer was used to obtain XRD spectra to determine the surface nature of adsorbents. Standard ASTM methods were followed for proximate analysis.

Batch adsorption and optimization

A three factor with four level Taguchi L16 orthogonal array was obtained using Minitab 18.0 to perform the experiments. The three factors are initial pH of the wastewater (1.5, 3, 4.5, 6), dose (0.1, 0.4, 0.7, 1.0 g 50mL⁻¹), and contact time (30, 60, 90, 240 min) (Table I). For batch adsorption, a fixed amount of HNGAC was added to 250 ml of wastewater in an Erlenmeyer flask and kept in an orbital shaker for a defined time at 30°C and 100 rpm. The Pb(II) concentration of the filtered effluent was analyzed using an atomic absorbance spectroscope (ECIL, India). Experimental runs were performed in duplicate and average values were reported. Equation (1) and (2) were used to determine the removal of Pb(II) and the uptake capacity of the adsorbent, respectively

$$\% \text{ Removal of Pb(II)} = \frac{C_o - C_e}{C_o} \times 100 \quad (1)$$

$$q_e = \frac{(C_o - C_e)V}{m} \quad (2)$$

where, C_o and C_e are the initial and final concentration of Pb(II) in the effluent, respectively. V is volume of effluent and m is mass of adsorbent.

Taguchi analysis, which uses a signal-to-noise ratio (SNR), was used to optimize the parameters and determine the optimal levels and their contribution to achieving the desired response.¹⁶ SNR analysis utilizes three response

characteristic functions based on the minimization, maximization, and nominalization of the responses.¹⁷ In this study, a larger-the-better characteristic function was used for SNR analysis since the goal was to recover Pb(II), as represented by equation (3)

Table I. Batch adsorption parameters and their levels.

Factor	Name	Level 1	Level 2	Level 3	Level 4
<i>P</i>	pH	1.5	3.0	4.5	6.0
<i>D</i>	Dose, g 50mL ⁻¹	0.1	0.4	0.7	1.0
<i>T</i>	Time, min	30	60	90	240

$$\left(\frac{S}{N}\right)_{\text{Larger is better}} = -10 \log \left[\frac{1}{n} \sum_{i=1}^n \frac{1}{y_i^2} \right] \quad (3)$$

where y_i is responses and n is the number of experiments performed. The response factors were optimized using Minitab version 18.1. Significance and effect level of the various factors in batch adsorption study was determined using ANOVA analysis.

RESULTS AND DISCUSSION

Characterization

Figure 1 shows a comparison of the FTIR spectra of GAC and HNGAC. After the alteration, the intensity of the surface functional group O-H, which corresponds to peak 3441 cm⁻¹ in GAC, increased and is shown by peak 3448 cm⁻¹ in HNGAC. The signal 2926 cm⁻¹ in GAC indicates the presence of less strong methyl and methylene groups (vibrational C-H bond). These C-H groups were oxidised and vanished from the HNGAC spectra following modification. It is evident that following modification, the peak at about 1630 cm⁻¹ in GAC, which is attributed to C=O groups, became noticeably more intense in HNGAC. The small peak in both spectra at around 1400 cm⁻¹ could be due to the presence of groups -CH₂ and -CH₃. The peaks in the 1000–1200 cm⁻¹ area can be attributed to the vibration of the C–O stretching and O–H bending in ether, lactonic, and phenol. The peak in the HNGAC spectra at 607.50 cm⁻¹ may be due to freshly formed surface groups of oxygen and nitrogen-containing groups.¹⁸⁻²¹

Comparison in FTIR spectra of GAC and HNGAC can be observed in Fig. 1. Surface functional group O-H corresponds to peak 3441 cm⁻¹ in GAC and its intensity has been increased after the modification and can be presented by the peak 3448 cm⁻¹, This indicating the enhancement in the OH surface groups as compared to GAC. In GAC, less intense methyl and methylene groups (vibrational C-H bond) were available and can be presented by the peak 2926 cm⁻¹. After modification these C-H groups were oxidized and disappeared in HNGAC spectra. It can be seen that peak around 1630 cm⁻¹, which can be assigned to C=O groups, was significantly intensified after modification. The existence of groups -CH₂ and -CH₃ may be the cause of the little peak in all spectra at about 1470 cm⁻¹. The

vibration of the C-O stretching and O-H bending in ether, lactonic, and phenol can be referred to the peaks in the 1000–1200 cm^{-1} region. Similarly, newly produced surface groups of oxygen and nitrogen-containing groups could be accountable for the peaks in the HNGAC spectrum at 607.50 cm^{-1} and close to 1100 cm^{-1} .

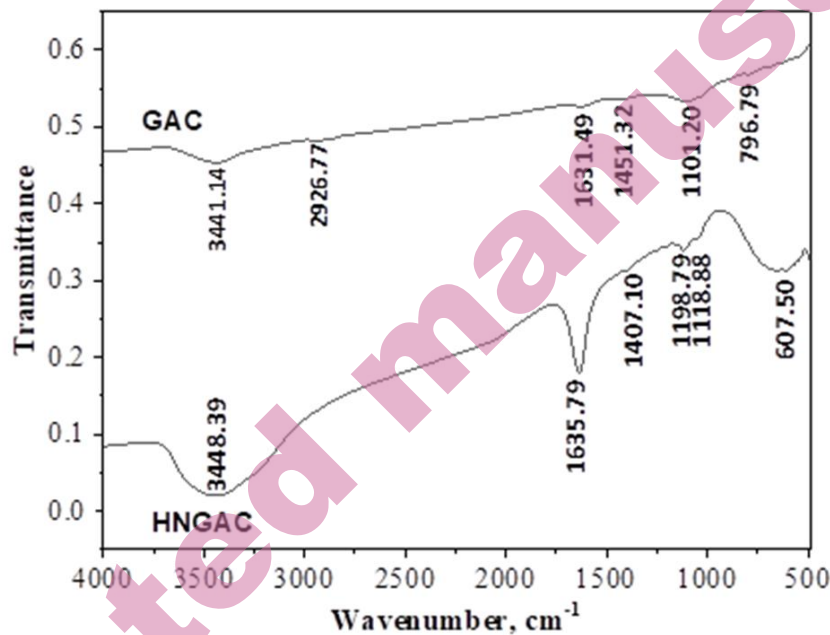


Fig. 1. FTIR spectra of GAC and HNGAC for the wavelength 500–4000 cm^{-1} .

In Fig. 2, SEM micrographs of GAC and HNGAC are presented. GAC has an irregular porosity structure and a rough surface. Acid treatment with nitric acid decreased the internal micropores of GAC and removed impurities from its surface. Because nitric acid is a potent oxidant, the acid treatment created canal-like mesopores on the surface, which reduced the pore volume and surface area.^{22,23} The impregnation of nitric acid reduced the microporous pore volume and specific surface area of the activated carbon, as found by Jiang *et al.*²⁴ EDS elemental analysis showed that impurities of GAC were removed and oxygen-containing groups were increased after acid treatments. Moreover, HNGAC was found to contain nitrogen, indicating that nitrogen-containing groups were formed on the surface after modification.

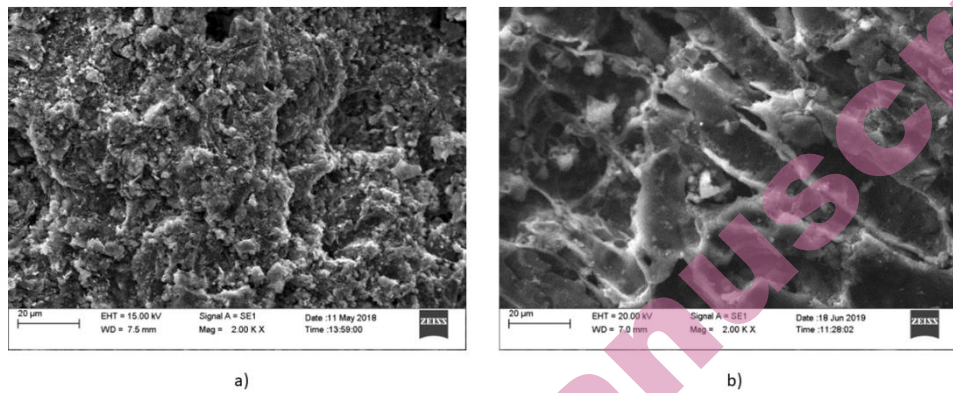


Fig. 2. Surface morphology image of (a) GAC and (b) HNGAC obtained by SEM.

The crystalline or amorphous character of GAC and HNGAC was determined using the XRD spectra shown in Fig. 3. The peaks at 26 and 42 correspond to 002 and 100 diffraction surfaces, respectively, and signify the amorphous nature of activated carbon. The diffraction pattern of HNGAC exhibited several diffraction peaks, showing an increase in crystallinity due to modification. Similar effects of HNO_3 modification on adsorbent prepared from the waste of olive tree prune were observed by Calero *et al.*²⁵

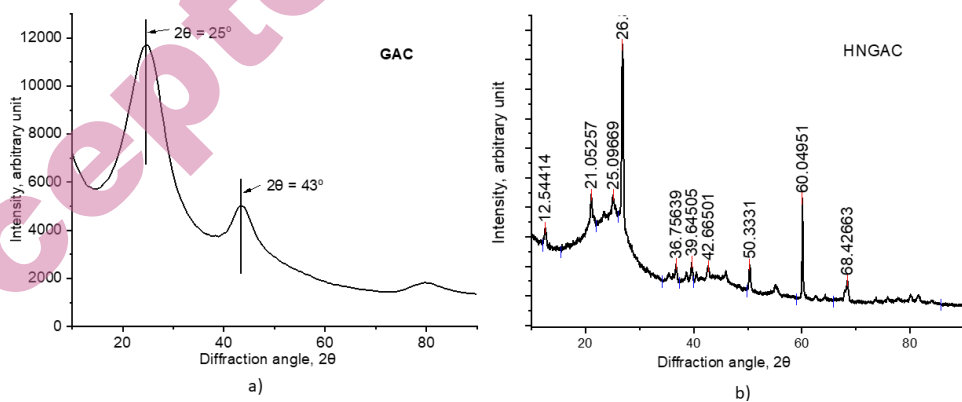


Fig. 3. XRD spectra of (a) GAC and (b) HNGAC at the diffraction angle 0-90°

Taguchi optimization

Three parameters at four different levels were used in batch adsorption research using the Taguchi L16 orthogonal array. Table II displays the results for each run's adsorbent capacity, and Fig. 4 displays the mean signal-to-noise ratio (SNR) plot for every variable associated with HNGAC's uptake capacity. It was

found that while the SNR value decreased with increasing dose, it increased with increasing pH and time. At $P4-D1-T4$, the mean SNR value was greatest. The ideal factor values were found to be pH 6, adsorbent dose of 0.05 g, and time of 240 minutes, based on the maximization feature of SNR. Nonetheless, there was little difference in uptake capacity for pH values of 4.5 and 6, so a pH value of 4.5 could be selected from an economic perspective for both adsorbents. The *SNR* analysis revealed that pH was the highly influential factor in the adsorption of lead onto HNGAC.

Table II. Taguchi experimental run for adsorption of lead onto HNGAC and response (adsorbent uptake capacity).

Exp. No.	P (pH)	D (Dose / g)	T (Time/ min)	q_e / mg g ⁻¹
1	$P1$	$D1$	$T1$	0.12
2	$P1$	$D2$	$T2$	0.21
3	$P1$	$D3$	$T3$	0.20
4	$P1$	$D4$	$T4$	0.21
5	$P2$	$D1$	$T2$	2.38
6	$P2$	$D2$	$T1$	1.31
7	$P2$	$D3$	$T4$	0.95
8	$P2$	$D4$	$T3$	0.77
9	$P3$	$D1$	$T3$	9.43
10	$P3$	$D2$	$T4$	5.74
11	$P3$	$D3$	$T1$	3.18
12	$P3$	$D4$	$T2$	2.92
13	$P4$	$D1$	$T4$	9.93
14	$P4$	$D2$	$T3$	5.92
15	$P4$	$D3$	$T2$	3.96
16	$P4$	$D4$	$T1$	2.54

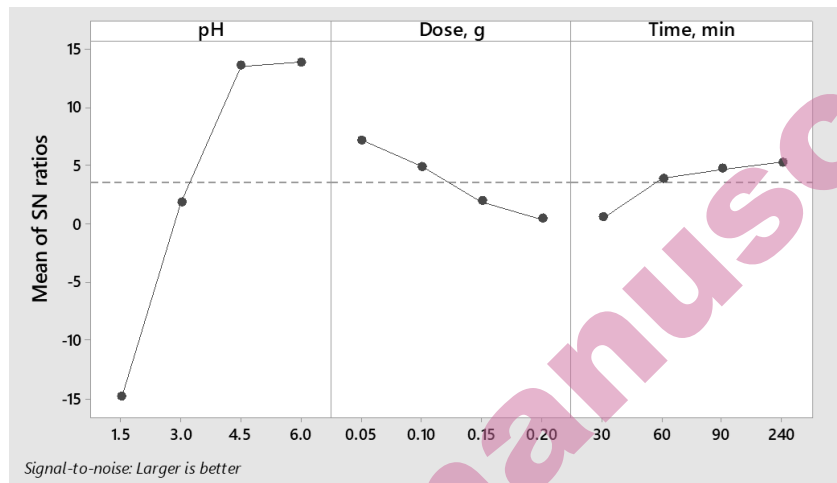


Fig. 4. Signal to noise ratio plot for removal capacity of HNGAC for pH, dose, and time at different level.

To determine the significance level of factors on the adsorbent uptake capacity, an analysis of variance (ANOVA) was carried out and presented in Table III. As observed coefficient of determination (R^2) was found 95.71, which signifies that the ANOVA model fitted well to the data. The ratio of variance between samples to variance within samples is termed as F-value and it indicates the parameters which affect the response largely. The initial pH of the effluent was found to have the highest significance on adsorption of lead onto HNGAC with F -value of 28.07 and lowest significant factor is adsorbent dose with F -value of 0.007.

Table III. ANOVA analysis for adsorption of lead onto HNGAC.

Source	DF	SS	MS	F-Value	P-Value
pH	3	90.629	30.210	28.07	0.001
Dose/ g	3	35.563	11.854	11.01	0.007
Time/ min	3	17.743	5.914	5.50	0.037
Error	6	6.457	1.076		
Total	15	150.393			
R^2		R^2 (adj)			
95.71%		89.27%			

Effect of each factor

The effect of pH on the adsorption of Pb(II) by HNGAC is shown in Fig. 5. The pH of the effluent has a significant impact on the adsorption process, affecting the charge on the surface and the ionization of Pb(II) in the effluent. To investigate

this, the pH was varied from 1.5 to 6, as Pb(II) tends to precipitate at basic pH.²⁶ At low value of pH, Pb(II) and H⁺ ions compete to be adsorbed on HNGAC and consequently result in slow adsorption. Increasing the initial pH of the effluent led to an increase in the uptake capacity of HNGAC, as the competition between hydrogen and lead ions decreased for the adsorption sites. Pb(II) ions were then able to bond with functional groups like -OH and -COOH present on the adsorbent surface.^{26,27} Moreover, at high pH the negative charge on the surface was increased, as proton gets removed from the functional groups present at the surface, this results in enhanced electrostatic forces of attraction for Pb(II) improving the adsorption.²⁸

According to the results presented in Fig. 5, an increase in adsorbent dose led to a decrease in the uptake capacity of Pb(II). The reason behind this trend may be the existence of either unsaturated adsorption sites or the overlapped and aggregated sites due to the maximum adsorption reached at a certain dose of adsorbent.²⁹

The effect of contact time on Pb(II) uptake capacity was investigated, and as shown in Fig. 5, the uptake increased up to 90 minutes, after which it reached a plateau. This trend could be attributed to the initial availability of more than enough active sites for the adsorption of Pb(II), which became occupied over time, resulting in effective utilization of the adsorbent. As the number of active sites decreased with time, the competition between the lead ions in the effluent and the adsorbent surface for relatively fewer sites slowed down the adsorption process.

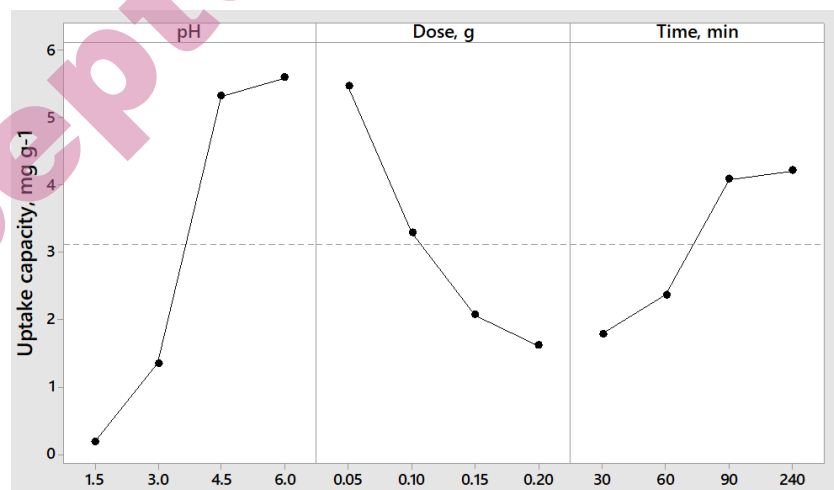


Fig. 5. Effect of initial pH, adsorbent dose, and contact time on adsorption performance of HNGAC for the removal of Pb(II).

Fig. 6 displays response surface plots that illustrates the impact of two factors on the adsorption. Fig. 6(a) indicates that, to achieve optimal adsorbent capacity, adsorbent dose should be less than $0.1 \text{ g } 50\text{mL}^{-1}$, and the pH level should be more than 4. This suggests that competition between Pb(II) and H^+ ions was reduced at higher pH, and that complete saturation of adsorption sites occurred at lower adsorbent doses. It can be found from Fig. 6(b) that higher adsorbent capacity is obtained at $\text{pH} > 4.5$ and $\text{time} > 80 \text{ minutes}$. This implies that insufficient interaction between the lead ions and adsorbent sites prevented high absorption capacity from being reached at the start of adsorption, even at high pH. High lead uptake capacity of HNGAC was achieved at dose $< 0.1 \text{ g } 50\text{mL}^{-1}$ and $\text{time} > 90 \text{ min}$ as can be observed in Fig. 6(c).

Fig. 6. Plots of simultaneous effect of two factors on lead adsorption onto HNGAC (a) initial pH and Dose (b) time and pH, and (c) time and dose.

Isotherm study

The fitting graphs for the Langmuir and Freundlich models of the experimental data for Pb(II) adsorption onto HNGAC are shown in Fig. 7. Table IV displays the parameters of isotherm models that were derived from fitting experimental data. The correlation coefficient (R^2) of the Langmuir model is higher than that of the Freundlich model. This shows that the adsorption equilibrium data are fitted well to the Langmuir equation, and the adsorption involved monolayer adsorption. Maximum monolayer adsorption capacity obtained from the Langmuir model is 9.93 mg g^{-1} for HNGAC.

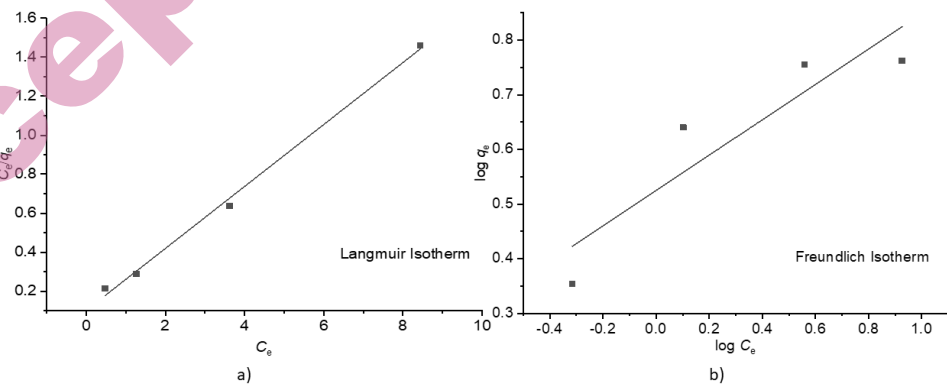


Fig. 7. Plot of isotherm study (a) Langmuir isotherm (b) Freundlich isotherm HNGAC ($\text{pH} = 4.5$; time-60 min; speed-100 rpm; volume- 50 mL; temperature-30 °C; dose-2 g L $^{-1}$).

Table IV Parameters for the isotherm models for adsorption onto HNGAC.

Langmuir			Freundlich		
$q_m /$ mg g^{-1}	$K_L /$ L mg^{-1}	R^2	$1/n$	$K_F /$ $\text{mg g}^{-1} ((\text{mg L}^{-1})^{1/n})^{-1}$	R^2
9.90099	0.639240506	0.99	0.323	1.688769234	0.836

Kinetic study

Both pseudo-first-order and pseudo-second-order kinetic models were used to assess the adsorption of Pb(II) onto HNGAC. Fig. 8 displays kinetic graphs, while Table 4 provides the correlation coefficient and kinetic model parameter. Because of its higher correlation coefficient of 0.99, the pseudo-second-order kinetic model is shown to better describe the adsorption kinetics than the pseudo-first-order. This implies that chemical adsorption may potentially be used to regulate the adsorption process. Compared to the pseudo-first-order model, the value of q_e derived from the pseudo-second-order model agrees better with the value of q_e found empirically. Abbaszadeh *et al.* (2016) observed similar outcomes for the adsorption of Pb(II) on activated carbon from papaya peel biowaste.²⁶ They found the measured uptake capacity of 38.31 mg g⁻¹ and calculated uptake capacity of 42.55 mg g⁻¹ from pseudo-second-order kinetic.

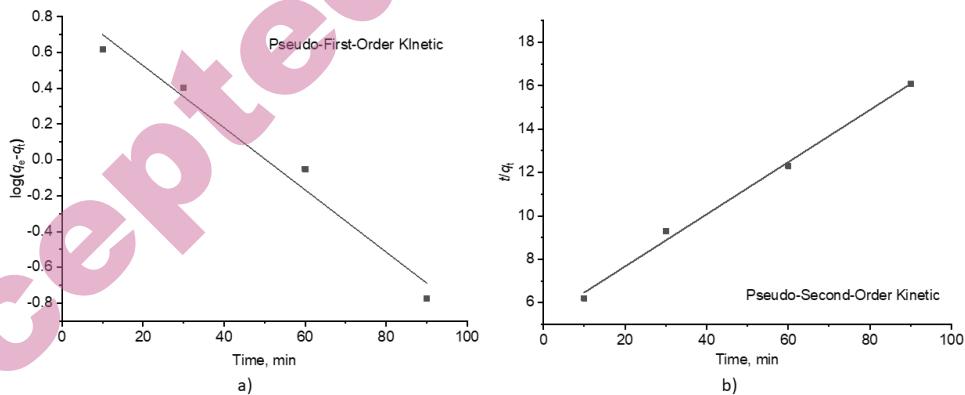


Fig. 8. Kinetic study graph for lead adsorption onto HNGAC (a) Pseudo-first-order model (b)Pseudo-second-order model (initial pH-4.5; adsorbent dose-0.1 g 50mL⁻¹; concentration- 10.2 mg L⁻¹).

Table V Kinetic equation parameter for adsorption onto HNGAC for the PFO and PSO models.

PFO			PSO		
K_1 / h^{-1}	q_e	R^2	$K_2 / \text{g mg}^{-1}\text{h}^{-1}$	q_e	R^2
0.039151	2.394082	0.973	0.002738684	8.333333	0.994

Mechanism of adsorption

The adsorption of Pb(II) onto the adsorbents involve physical and chemical interactions with the surface functional groups. The adsorption of Pb(II) may be caused by ion exchange interactions with surface groups like hydroxyl and carboxyl. The FTIR analysis revealed that the intensity of groups, especially –OH and –COOH, was higher in HNGAC compared to GAC, which supports the ion exchange between adsorbent and adsorbate. It was also observed that the amount of Pb(II) uptake by HNGAC was significantly higher than GAC, indicating that chemisorption played a major role in the adsorption process rather than physisorption. Impregnation of GAC with HNO₃ considerably improved the negative surface charge of the adsorbent, which attracted the lead ions.

CONCLUSIONS

Pb(II) was separated from effluent of LAB recycling unit utilizing HNGAC as an adsorbent. The intensity of the -OH and -COOH functional groups present at the surface of GAC are found to be increased after the process of modification with nitric acid, moreover some new nitrogen containing functional groups were formed after modification. Modification led to increase in mesopores and decrease in micropores. The optimum level of parameters found using Taguchi analysis, was, time 240 min, pH 6 and adsorbent dose 0.05 g 50mL⁻¹. The maximum adsorption capacity of GAC found to be increased due to modification from 7.69 mg g⁻¹ to 9.93 mg g⁻¹. From isotherm and kinetic studies, it can be conferred that adsorption of lead onto HNGAC follows the Langmuir isotherm and pseudo second order kinetics. Adsorption of lead onto HNGAC include monolayer adsorption followed by the chemical interaction with functional groups available on the adsorbent surface. Overall, it could be established that, adsorption can be used as an effective technique for the remediation of lead from wastewater of lead-acid battery recycling unit and HNGAC could be used as an efficient adsorbent.

Acknowledgements: The authors want to acknowledge the support and facilities provided by National Institute of Technology Raipur, India. The author also wants to acknowledge the Guru Ghasidas University Bilaspur, India for granting the study leave to do Ph.D.

И З В О Д

АДСОРПЦИОНО УКЛАЊАЊЕ Pb(II) ИЗ ИНДУСТРИЈСКОГ ЕФЛУЕНТА ПРИМЕНОМ
АКТИВНОГ УГЉА МОДИФИКОВАНОГ АЗОТНОМ КИСЕЛИНОМ: ОПТИМИЗАЦИЈА
ПРИМЕНОМ ТАГУЧИ МЕТОДЕ

SAURABH MESHRAM¹, ANURADHA N JOSHI¹, GAUTAM PRASAD DEWANGAN¹, CHANDRAKANT THAKUR² AND
ANUPAM B. SONI²

¹Department of Chemical Engineering, Guru Ghasidas Vishwavidyalaya, Bilaspur, 495009, Chhattisgarh, India, ²Department of Chemical Engineering, National Institute of Technology Raipur, 492010, Chhattisgarh, India.

Циљ ове студије био је испитивање примене гранулисаног активног угља модификованим азотном киселином за третман отпадних вода из постројења за рециклажу оловно-киселинских акумулатора, ради уклањања олова. Адсорбенс је окарактерисан применом FTIR, SEM и XRD анализа. Модификацијом су промењене површинске функционалне групе, површинска морфологија и кристаличност. Шаржна адсорпција испитивања спроведена су ради процене утицаја дозе адсорбенса, почетне pH вредности и контактног времена на ефикасност адсорпције уклањања олова. Експерименти су изведени у складу са Тагучи методом дизајна експеримената, а фактори су оптимизовани на основу анализе односа сигнала/шума (SNR) у циљу максимизације одзива. Оптималне вредности фактора утврђене су као pH 6, доза адсорбенса од 0,05 g и време од 240 минута за адсорпцију олова на адсорбенс, при чему је адсорпциони капацитет износио $9,93 \text{ mg g}^{-1}$. На основу ANOVA анализе, pH је идентификован као најзначајнији фактор, са F-вредношћу од 28,07. Изотермска и кинетичка испитивања такође су спроведена ради разумевања механизма адсорпције. Утврђено је да адсорпција прати Лангмуирову изотерму и кинетички модел другог реда.

(Примљено 19. августа; ревидирано 22. октобра; прихваћено 25. децембра 2025.)

REFERENCES

1. S. Meshram, R. S. Thakur, G. Jyoti, C. Thakur, A. B. Soni, *J. Indian Chem. Soc.* **99** (2022) 100469 (<https://doi.org/10.1016/j.jics.2022.100469>)
2. M. Caccin, M. Giorgi, F. Giacobbo, M. D. Ros, L. Besozzi, M. Mariani, *Desalin. Water Treat.* **57** (2016) 4557 (<https://doi.org/10.1080/19443994.2014.992974>)
3. S. Meshram, C. Thakur, A. B. Soni, *J. Serb. Chem. Soc.* **85** (2020) 953 (<https://doi.org/10.2298/JSC191103015M>)
4. S. Meshram, S. Dharmadhikari, R. S. Thakur, *C. Thakur, A. B. Soni, J. Hazard. Mater. Adv.* **10** (2023) 10297 (<https://doi.org/10.1016/j.hazadv.2023.100297>)
5. C. Thakur, I. D. Mall, V. C. Srivastava, *Theor. Found. Chem. Eng.* **48** (2014) 60. (<https://doi.org/10.1134/S004057951401014X>)
6. C. P. Dwivedi, J. N. Sahu, C. R. Mohanty, B. R. Mohan, B. C. Meikap, *J. Hazard. Mater.* **156** (2008) 596 (<https://doi.org/10.1016/j.jhazmat.2007.12.097>)
7. J. P. Chen, X. Wang, *Sep. Purif. Technol.* **19** (2000) 157. ([https://doi.org/10.1016/S1383-5866\(99\)00069-6](https://doi.org/10.1016/S1383-5866(99)00069-6))
8. M. A. E. Franco, C. B. Carvalho, M. M. Bonetto, R. P. Soares, L. A. Féris, *J. Clean. Prod.* **161** (2017) 947 (<https://doi.org/10.1016/j.jclepro.2017.05.197>)
9. A. H. Sulaymon, D. W. Aboot, A. H. Ali, *Hydrol. Curr. Res.* **2** (2011) 1000120 (<http://dx.doi.org/10.4172/2157-7587.1000120>)
10. A. Jusoha, L. S. Shiungb, N. Alia, M. J. M. M. Noor, *Desal.* **206** (2007) 9 (<https://doi.org/10.1016/j.desal.2006.04.048>)
11. K. Wang, J. Zhao, H. Li, X. Zhang, H. Shi, *J. Taiwan Inst. Chem. Eng.* **61** (2016) 287 (<https://doi.org/10.1016/j.jtice.2016.01.006>)
12. H. J. Fan, P. R. Anderson, *Sep. Purif. Technol.* **45** (2005) 61 (<https://doi.org/10.1016/j.seppur.2005.02.009>)
13. S. Yao, J. Zhang, D. Shen, R. Xiao, S. Gu, M. Zhao, J. Liang, *J. Colloid Interf. Sci.* **463** (2016) 118 (<https://doi.org/10.1016/j.jcis.2015.10.047>)
14. Z. Jiang, Y. Liu, X. Sun, F. Tian, F. Sun, C. Liang, W. You, C. Han, C. Li, *Langmuir* **19** (2003) 731 (<https://doi.org/10.1021/la020670d>.)

15. A. M. El-Wakil, W. M. Abou El-Maaty, F. S. Awad, *J. Anal. Bioanal. Tech.* **5** (2014) 1000187 (<https://doi.org/10.4172/2155-9872.1000187>)
16. M. Nandhini, B. Suchithra, R. Saravanathanthamizhan, D. G. Prakash, *J. Electrochem. Sci. Eng.* **4** (2014) 227 (<https://doi.org/10.5599/jese.2014.0056>)
17. S. Meshram, C. Thakur, A. B. Soni, *Pollution* **6** (2020) 879 (<https://doi.org/10.22059/poll.2020.302442.808>)
18. M. A. Ramos, V. G. Serrano, C. V. Calahorro, A. J. L. Peinado, *Spectrosc. Lett.* **26** (1993) 1117 (<https://doi.org/10.1080/00387019308011598>)
19. V. G. Serrano, M. A. Ramos, A. J. L. Peinado, C. V. Calahorro, *Thermochimica Acta* **291** (1997) 109 ([https://doi.org/10.1016/S0040-6031\(96\)03098-5](https://doi.org/10.1016/S0040-6031(96)03098-5))
20. V. C. Srivastava, I. D. Mall, I. M. Mishra, *J. Hazard. Mater.* **134** (2006) 257 (<https://doi.org/10.1016/j.hazmat.2005.11.052>)
21. T. S. Anirudhan, S. S. Sreekumari, *J. Environ. Sci.* **23** (2011) 1989 ([https://doi.org/10.1016/S1001-0742\(10\)60515-3](https://doi.org/10.1016/S1001-0742(10)60515-3))
22. N. A. Kolur, S. Sharifian, T. Kagnazchi, *Turkish J. Chem.* **43** (2019) 663 (<https://doi.org/10.3906/kim-1810-63>)
23. M. Dutta, S. Mishra, M. Kaushik, J. K. Basu, *Res. J. Environ. Sci.* **5** (2011) 741 (<https://doi.org/10.3923/rjes.2011.741.751>)
24. X. Jiang, X. Lan, Y. Song, X. Xing, H. M. A. Hassan, *J. Chem.* (2019) 8593742 (<https://doi.org/10.1155/2019/8593742>)
25. M. Calero, A. Pérez, G. Blázquez, A. Ronda, M. A. M. Lara, *Ecol. Eng.* **58** (2013) 344 (<https://doi.org/10.1016/j.ecoleng.2013.07.012>)
26. S. Abbaszadeh, S. R. W. Alwi, C. Webb, N. Ghasemi, I. I. Muhamad, *J. Clean. Prod.* **118** (2016) 210 (<https://doi.org/10.1016/j.jclepro.2016.01.054>)
27. Z. Guo, J. Zhang, Y. Kang, H. Liu, *Ecotoxicol. Environ. Saf.* **145** (2017) 442 (<https://doi.org/10.1016/j.ecoenv.2017.07.061>)
28. Y. Li, Q. Du, X. Wang, P. Zhang, D. Wang, Z. Wang, Y. Xia, *J. Hazard. Mater.* **183** (2010) 583 (<https://doi.org/10.1016/j.hazmat.2010.07.063>)
29. S. Meshram, C. Thakur, A. B. Soni, *Indian Chem. Eng.* **63** (2020) 460 (<https://doi.org/10.1080/00194506.2020.1795933>)